EMBEDDED SELF-SHIELDING METHOD APPLIED TO DOUBLY HETEROGENEOUS FULLY CERAMIC MICRO-ENCAPSULATED FUELS

Kang Seog Kim, Jianwei Hu*
Oak Ridge National Laboratory, 1 Bethel Valley Rd., P.O. Box 2008, Oak Ridge, Tennessee 37831
kimk1@ornl.gov; huj1@ornl.gov

Cole A. Gentry
The University of Tennessee, Department of Nuclear Engineering, 311 Pasqua Engineering Building, Knoxville, Tennessee 37996-2300
gentryca@ornl.gov

ABSTRACT

This research focuses on the development of a new fast and robust lattice physics methodology for modeling and simulation of doubly heterogeneous (DH) nuclear fuels containing tristructural isotropic (TRISO) coated fuel particles and fully ceramic micro-encapsulated (FCM) fuel. The specific aims of this study are to determine if existing complex methods for DH calculations can be integrated with the Embedded Self-Shielding Method (ESSM) developed at Oak Ridge National Laboratory ORNL. New ESSM methodologies for the DH resonance self-shielding calculation have been developed using the Sanchez and Pomraning's method. These methodologies have been incorporated into a transport lattice code based on method of characteristics (MOC) for spatial discretization. Benchmark problems including reference solutions have been developed to validate new DH lattice physics methodology. Benchmark results show that new DH capability for resonance self-shielding and eigenvalue calculations is working reasonably.

Key Words: **Double heterogeneity, ESSM, method of characteristics, FCM**

1. INTRODUCTION

In current nuclear reactors, the fuel is typically composed of fissile material encased in cladding and surrounded by coolant. This type of fuel is sometimes called a singly heterogeneous fuel. In doubly heterogeneous (DH) fuel, many tiny fuel particles coated with thin layers of protective materials are randomly dispersed throughout a graphite matrix, which is then formed into a sphere, cylinder, or prismatic cylinder. Many of these graphite matrix bodies are arranged in a lattice in the reactor core, creating two levels of heterogeneity in the fuel. These particulate fuels could significantly improve the safety and nonproliferation characteristics of reactors; they also are an attractive alternative to conventional nuclear fuel for next generation nuclear power plants. Particulate fuels have been used in the prismatic and pebble bed high temperature gas cooled reactors (HTGRs) with tri-structural isotropic (TRISO) fuel. Current studies for accident-tolerant fuels in light water reactors (LWRs)

call for the use of fully ceramic micro-encapsulated (FCM) fuel [1]. FCM fuel is also being proposed for fluoride-salt high temperature reactors.

Doubly heterogeneous fuels challenge the current methods used for physics analysis of reactor and fuel cycle systems. In principle, continuous energy Monte Carlo calculations that explicitly represent the thousands of tiny grains in the graphite matrix could be used for DH fuel calculations. However, this method is not effective for modeling time-dependent depletion of the isotopics in each particle, entailing extensive computational resources for routine parametric studies that typically require hundreds of runs. A fast-running multigroup (MG) lattice physics method is needed to enable the scoping studies and parametric evaluations required to assess the performance of TRISO-based fuel designs in current and advanced reactor systems. Currently there are few nuclear modeling software tools that can adequately address the DH resonance self-shielding of the MG nuclear cross section data for TRISO and FCM fuels. In addition, simulation of a reactor's fuel performance requires a methodology to treat depletion of the fuel coupled with the resonance self-shielding. Oak Ridge National Laboratory (ORNL) recently developed a new transport lattice physics methodology that uses an improved self-shielding approach called the Embedded Self-Shielding Method (ESSM) [2,3], coupled with the Method of Characteristics (MOC) for solving the neutron transport equation. The new methodology is faster in computing time than previous methods, but its applicability is limited to conventional LWR fuel. Expanding this new method to DH particulate fuels would provide a fast and robust lattice physics tool to evaluate the impact of new TRISO and FCM fuel designs on current and future reactors.

Sanchez and Pomraning [4–7] have developed a complex method for DH calculations that treats neutron transport through a stochastic mixture of grains using the MOC algorithm. Since the new ORNL lattice physics method also uses a MOC transport solution, the Sanchez and Pomraning approach is attractive. However, theoretical advancements and modifications to the original method are required to make the approach compatible with the new ESSM self-shielding method developed by ORNL.

In this study, new ESSM methodologies for the DH self-shielding calculation were developed, followed by development of DH subroutines for resonance self-shielding and eigenvalue calculations. These subroutines have been integrated with a transport lattice code. Benchmark problems including reference solutions have been developed to validate new DH lattice physics methodology. The benchmark calculations have been performed using an inhouse transport code with the ESSM and the subgroup methods and then compared to the reference solutions.

2. DESCRIPTION OF METHOD

2.1 Embedded Self-Shielding Method for DH

ESSM has been developed for the resonance self-shielding calculation and applied only to single heterogeneity problems. This method requires fixed source transport calculations for estimating background cross sections. ESSM is a new resonance treatment methodology that has never been applied to DH cases. When estimating resonance self-shielded cross section by ESSM, absorption

cross sections ($\Sigma_{i,a,g}$) in the fuel and cladding are iteratively determined by solving the fixed source transport Equation (1) which can be rewritten in Equation (2).

$$\hat{\Omega}\cdot\nabla\varphi_g(\hat{\Omega}_m)+\sum_j(\Sigma_{j,a,g}+\lambda_{j,g}\Sigma_{j,p})\varphi_g(\hat{\Omega}_m)=\sum_j\lambda_{j,g}\Sigma_{j,p}\,, \tag{1}$$

$$\hat{\Omega}\cdot\nabla\varphi_g(\hat{\Omega}_m)+\Sigma_{t,g}\varphi_g(\hat{\Omega}_m)=S_g\,, \tag{2}$$

where φ_g is an angular flux of group g, $\Sigma_{j,a,g}$ is a macroscopic absorption cross section of nuclide j, $\Sigma_{j,p}$ is a macroscopic potential cross section, Ω_m is a neutron direction and $\lambda_{j,g}$ is an intermediate resonance parameter. The same ESSM equation can be applied to the DH problems. However, when solving Equation (2), total cross section ($\Sigma_{t,g}$) and source (S_g) for the DH material zones should be re-estimated to be effective. When solving the ESSM MOC equation for the DH problem, outgoing and average angular fluxes should be obtained by using different equations from the conventional MOC equations, which is discussed in Section 2.2 in detail. The average scalar flux at a flat source region i can be obtained by using Equation (3), as follows:

$$\phi_{i,g}=\sum_m w_m\overline{\varphi}_{i,g,m}\,, \tag{3}$$

where w_m denotes quadrature weight of angle m. The corresponding macroscopic and microscopic background cross sections can be obtained by using the following Equation (4).

$$\Sigma_{i,b,g}=\frac{\Sigma_{i,a,g}\phi_{i,g}}{1-\phi_{i,g}}\quad\rightarrow\quad\sigma^j_{i,b,g}=\frac{\Sigma_{i,b,g}}{N_{i,j}}\,. \tag{4}$$

Self-shielded absorption cross sections for each nuclide can be read from the resonance self-shielded cross section table. The absorption cross sections are used to update $\Sigma_{j,a,g}$, after which the same ESSM calculation is performed. This iteration procedure is continued until the macroscopic background cross sections ($\Sigma_{i,b,g}$) are converged.

2.2 Sanchez and Pomraning's method for MOC

Figure 1 illustrates a configuration of the FCM fuel compact in which TRISO particles are randomly distributed. This problem is to be solved by the Sanchez and Pomraning's method using MOC to estimate resonance self-shielded cross sections and to obtain multiplication factor and scalar flux. An overall algorithm for the DH treatment in MOC-based transport lattice code is shown in Figure 2. Since MOC should be used in both resonance fixed source and eigenvalue calculations, The DH module should be used for the ESSM fixed source and eigenvalue calculations.

By integrating the MOC solution and the analytic solution for the heterogeneous grain, the calculation sequence can be set for the stochastic medium as follows:

a. Various volumes (V, V_0, V_i, and V_{ik}^G) and volume fractions (p_0, p_i, p_{ik}, and p_{ik}^G) described in Figure 1 are calculated.

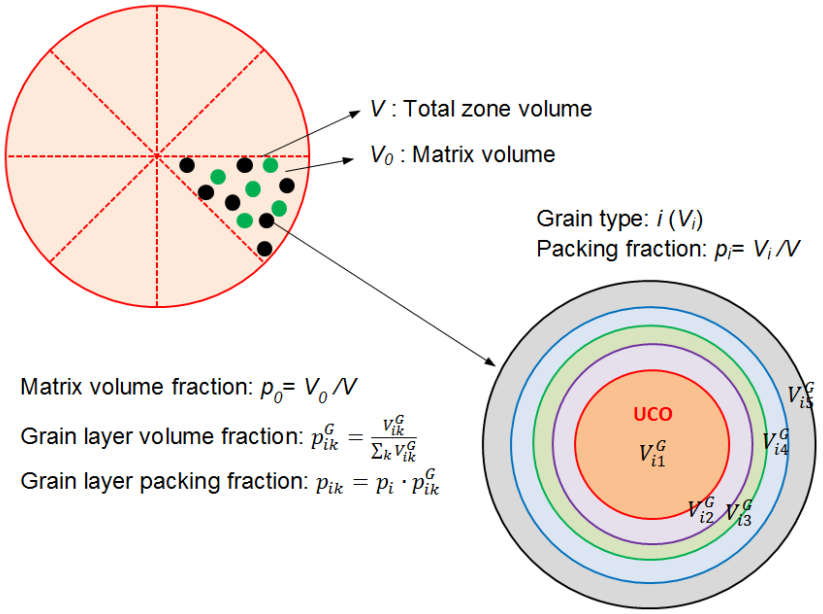

Figure 1. Configuration of fuel compact with TRISO particles.

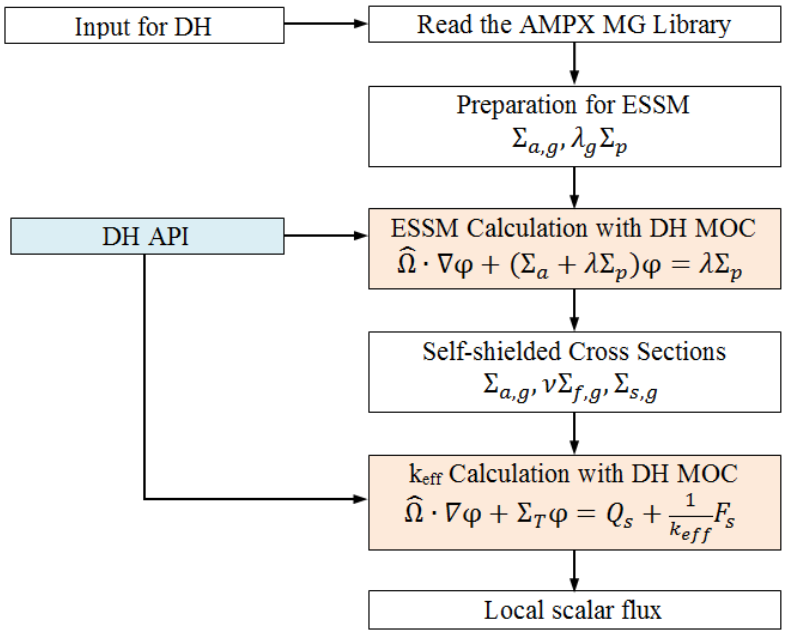

Figure 2. Overall algorithm for the DH treatment in transport lattice code.

b. The total cross section ($\Sigma_{t,ik}$) is processed, and the escape (E_{ik}^G) and collision probability ($P_{ik,il}^G$) are calculated at each layer. These are defined as follows:

$P_{ik,il}^G$ = probability for a source neutron originating from the l^{th} layer of the i^{th} grain type to have its first collision at the k^{th} layer of the i^{th} grain type

E_{ik}^{G} = probability for a source neutron originating from the k^{th} layer of the i^{th} grain type to escape through the grain boundary

c. Tilde total macroscopic cross sections ($\tilde{\Sigma}_{t,g}$) are calculated for a DH material zone by using Equation (5), in which the subscript g is the energy group. This is omitted in all equations for convenience. In Equation (5), $\Sigma_{t,0}$ is total macroscopic cross section for matrix.

$$\tilde{\Sigma}_t = \Sigma_{t,0} + \frac{1}{p_0}\sum_{i=1}^{I}\sum_{k=1}^{K} p_{ik}\Sigma_{t,ik}E_{ik}^{G} . \quad (5)$$

d. Effective total macroscopic cross sections ($\Sigma_{t,g}$) and reduced escape probability ($\hat{E}_{ik,g}^{G}$) are calculated for a DH material zone iteratively by using Equation (6).

$$\Sigma_t^{(n+1)} = \Sigma_{t,0} + \frac{1}{p_0}\sum_{i=1}^{I}\sum_{k=1}^{K} p_{ik}(\Sigma_{t,ik} - \Sigma_t^{(n)})\hat{E}_{ik}^{G} , \quad (6)$$

for ESSM, $\Sigma_{t,g} = \Sigma_{a,g} + \lambda_g\Sigma_p$,
for eigenvalue calculation, $\Sigma_{t,g} = \Sigma_{a,g} + \Sigma_{s,g}$.

e. The renormalization coefficient ($r_{c,g}$) is calculated for a DH material zone which can be unity for non–DH material zones by using Equation (7).

$$r_c = p_0 + \sum_{i=1}^{I}\sum_{k=1}^{K} p_{ik}\hat{E}_{ik}^{G} . \quad (7)$$

f. Asymptotic flux ($\varphi_{as,g}$) and effective source (q_g) are calculated for a DH material zone by using Equations (8) and (9).

$$\varphi_{as} = q_0 + \frac{1}{p_0}\sum_{i=1}^{I}\sum_{k=1}^{K} p_{ik}q_{ik}E_{ik}^{g} \Big/ \tilde{\Sigma}_t , \quad (8)$$

and

$$q = \varphi_{as}\Sigma_t . \quad (9)$$

For ESSM, $q_g = \lambda_g\Sigma_p$,
For eigenvalue calculation, $q_g = \sum_{g'}\Sigma_{s,g'g}\phi_{g'} + \frac{1}{k_{eff}}\chi_g\sum_{g'}\nu\Sigma_{f,g'}\phi_{g'}$.

g. The MOC-based ESSM and eigenvalue calculations are performed to estimate equivalence cross section (Σ_{ik}^{eq}) and to obtain the multiplication factor by using Equation (10), where

$$\hat{\Omega} \cdot \nabla \varphi_g(\hat{\Omega}_m) + \Sigma_{t,g} \varphi_g(\hat{\Omega}_m) = q_g \,. \tag{10}$$

In MOC, the outgoing angular flux (φ_{out}^m) at direction *m* can be calculated from the incoming angular flux (φ_{in}^m) by using Equation (11), where *L* denotes a track segment.

$$\varphi_{out}^m = \varphi_{in}^m + r_c(1 - e^{-\Sigma_t L})(\varphi_{as} - \varphi_{in}^m) \,. \tag{11}$$

Average angular ($\overline{\varphi}_0^m$) and scalar ($\overline{\phi}_0$) fluxes for the matrix can be calculated by using Equations (12) and (13), respectively:

$$\overline{\varphi}_0^m = \frac{\varphi_{in}^m - \dfrac{q}{\Sigma_t}}{\Sigma_t L}(1 - e^{-\Sigma_t L}) + \frac{q}{\Sigma_t} \tag{12}$$

$$\overline{\phi}_0 = \sum_m w_m \overline{\varphi}_0^m \tag{13}$$

Average scalar flux ($\overline{\phi}_{ik}$) of grain *i* at layer *k* can be reconstructed by using Equations (14) and (15).

$$\phi_{ik} = \frac{1}{V_{ik}^g \Sigma_{t,ik}} \sum_{l=1}^{K} V_{il}^g q_{il} P_{ik,il}^g \tag{14}$$

$$\overline{\phi}_{ik} = \hat{E}_{ik}^g \overline{\phi}_0 + (E_{ik}^g - \hat{E}_{ik}^g)\varphi_{as} + \phi_{ik} \tag{15}$$

For ESSM, equivalence cross sections (E_{ik}^{eq}) at each grain layer need to be calculated by using Equation (16), which is to be used in estimating self-shielded cross sections.

$$\Sigma_{ik}^{eq} = \frac{\Sigma_{t,ik}\overline{\phi}_{ik} - \lambda \Sigma_{p,ik}}{1 - \overline{\phi}_{ik}} \tag{16}$$

Conceptually, the subgroup method is very similar to ESSM except for its use of subgroup data. ESSM and the subgroup method for DH have been implemented to assess the capability differences in in-house MOC-based transport lattice code.

3. ANALYSIS AND RESULTS

3.1 Benchmark Problems

Benchmark problems have been developed based on the work of Hong 2013 [8] to validate a new DH treatment capability for doubly heterogeneous particulate fuels such as FCM. Tables 1–3 provide geometrical data for the TRISO and BISO particles, composition data, and fuel specification, respectively. Benchmark problems include 8 single pins and 8 fuel assembly cases with various TRISO packing fractions, fuel types, burnable poison, TRISO kernel sizes, and fuel

temperatures. Table 4 provides benchmark problems for fuel pins and assemblies. Two types of TRISO particles with radii of 460 and 610 μm have been tested. In burnable poison rods, the 385 μm BISO particles are mixed with the 460 μm TRISO particles, with packing fractions of 33.8 % for $UC_{0.5}O_{1.5}$ TRISO and 10.3 % for BISO. Two types of fuel materials have been tested for transuranics (TRU) and $UC_{0.5}O_{1.5}$ in which ^{235}U enrichment is 16.0 weight %. Fuel pin configurations including TRISO and BISO can be found in Figures 4.2–4.9 for pin power comparison.

Table 1. Material and geometry of the TRISO and BISO particles

TRISO			**BISO**	
Material	**Kernel radius (cm)**		**Material**	**Kernel radius (cm)**
	460 µm	**610 µm**		
Kernel	0.0250	0.0400	Kernel	0.0250
Buffer	0.0350	0.0500	Buffer	0.0350
IPyC	0.0385	0.0535	IPyC	0.0385
SiC	0.0420	0.0570		
OPyC	0.0460	0.0610		

Table 2. Composition data

Composition	**Density (g/cm^3)**	**Nuclide**	**AND* (#/cm-barn)**	**Nuclide**	**AND* (#/cm-barn)**
TRU	9.461	$^{nat.}C$	1.16787E-02	^{238}Pu	5.86381E-04
		$^{nat.}Si$	1.16849E-02	^{239}Pu	1.13400E-02
		^{16}O	3.53055E-02	^{240}Pu	4.26975E-03
		^{235}U	2.76335E-07	^{241}Pu	7.01993E-04
		^{238}U	3.82940E-05	^{242}Pu	1.27338E-03
		^{237}Np	9.71015E-04	^{241}Am	3.00169E-04
$UC_{0.5}O_{1.5}$	10.0	^{235}U	3.64662E-03	$^{nat.}C$	1.12572E-02
		^{238}U	1.88611E-02	^{16}O	3.37650E-02
Gd_2O_3 in BISO	7.407	^{154}Gd	5.35905E-04	^{158}Gd	6.12286E-03
		^{155}Gd	3.64662E-03	^{160}Gd	5.38985E-03
		^{156}Gd	5.04490E-03	^{16}O	3.69897E-02
		^{157}Gd	3.86221E-03		
Buffer	1.05	$^{nat.}C$	5.26881E-02		
IPyC/OPyC	1.90	$^{nat.}C$	9.53403E-02		
SiC	3.18	Graphite	4.77721E-02	^{29}Si	2.23096E-03
		^{28}Si	4.40602E-02	^{30}Si	1.48094E-03
Zr clad	6.45	$^{nat.}Zr$	4.25810E-02		
moderator	1.00	^{1}H	6.68884E-02	^{16}O	3.34443E-02

*Atomic number density

Table 3. Fuel specification

Component	Item		Dimension
17 × 17 fuel assembly	Pitch (cm) # of fuel rods / GT+IT tubes Rod pitch (cm)		22.0600 264 / 25 1.2860
Fuel pin	Fuel compact , SiC	Density (g/cm^3) Outer radius (cm)	3.18 0.4095
	Gap, O_2	Density (g/cm^3) Outer radius (cm)	0.01 0.4180
	Cladding, $^{nat.}$Zr	Density (g/cm^3) Inner radius (cm) Outer radius (cm)	6.45 0.4180 0.4750
Guide and instrument tube	Tube, $^{nat.}$Zr	Density (g/cm^3) Inner radius (cm) Outer radius (cm)	6.45 0.5500 0.6000

Table 4. Benchmark problems for fuel pins and assemblies

Type	Case	Fuel Temp. (K) (# of pins)	Packing Fraction (%)	Kernel Size (μm)	Fuel Content
Pin	A1	300/300	33.8/10.3	500/385	$UC_{0.5}O_{1.5}/Gd_2O_3$
	A2	300	40	500	$UC_{0.5}O_{1.5}$
	A3	300	40	500	TRU
	A4	900	30	500	TRU
	A5	900/600	33.8/10.3	500/385	$UC_{0.5}O_{1.5}/Gd_2O_3$
	A6	900	40	500	TRU
	A7	900	40	500	$UC_{0.5}O_{1.5}$
	A8	900	40	800	TRU
Assembly	B1	300 (264)*	40	500	$UC_{0.5}O_{1.5}$
	B2	900 (264)	40	500	$UC_{0.5}O_{1.5}$
	B3	300 (256)	40	500	$UC_{0.5}O_{1.5}$
		300/300 (8)	33.8/10.3	500/385	$UC_{0.5}O_{1.5}/Gd_2O_3$
	B4	900 (256)	40	500	$UC_{0.5}O_{1.5}$
		900/600 (8)	33.8/10.3	500/385	$UC_{0.5}O_{1.5}/Gd_2O_3$
	B5	300 (264)	40	500	TRU
	B6	900 (264)	40	500	TRU
	B7	300 (256)	40	500	TRU
		300/300 (8)	33.8/10.3	500/385	$UC_{0.5}O_{1.5}/Gd_2O_3$
	B8	900 (256)	40	500	TRU
		900/600 (8)	33.8/10.3	500/385	$UC_{0.5}O_{1.5}/Gd_2O_3$

3.2 Benchmark Results

Reference solutions for the benchmark problems have been obtained by continuous energy Monte Carlo calculations. Previous investigations showed that multiplication factors are dependent upon configurations of TRISO particles. Therefore, the MCNP [9] and SERPENT [10] calculations were performed first for a single pin problem case A2 with cubic-centered and random distributions, as shown in Figure 3.

(a) Cubic-centered (MCNP) (b) Random (SERPENT)

Figure 3. Configurations of TRISO particle distribution.

The computational results show a difference of 337 pcm reactivity between the MCNP cubic-centered model and the SERPENT random distribution model. This difference should come from clipping and random distribution effects. Therefore, the SERPENT random distribution models were chosen to be used to obtain reference solutions.

Benchmark calculations have been performed for the benchmark problems shown in Table 4 by using a MOC-based in-house transport lattice code with the ENDF/B-7.0 47-group and 190-group libraries based on the HELIOS energy group structures in which subgroup and ESSM are used for resonance self-shielding calculation. The reference solutions have been obtained by performing the continuous energy SERPENT calculations with the ENDF/B-7.0 cross section data.

Figure 4 and Table 5 compare the benchmark calculation results to the reference solutions, including pin power distributions, multiplication factors, and RMS and maximum errors of pin power distributions. Both DH-ESSM and DH-Subgroup predict the multiplication factors and power distributions precisely. About 100 pcm difference between DH-ESSM and DH-Subgroup might result from the quality of resonance data. It is also noted that DH-ESSM underestimates the multiplication factor compared to DH-Subgroup, which is very consistent with the prediction trend for singly heterogeneous fuels. This underestimation should come from the intrinsic resonance interference formula in which the effective background cross section would be increased, resulting in greater ^{238}U absorption for self-shielded cross sections. It should be noted that the results with the 47 g library are very consistent with the results in the 190 g library. Although the results have been generated for pressurized water reactors, they are working reasonably even for the FCM fuels. Figure 5 provides a comparison of neutron spectra between SERPENT and transport lattice code with ESSM which are very consistent with each other.

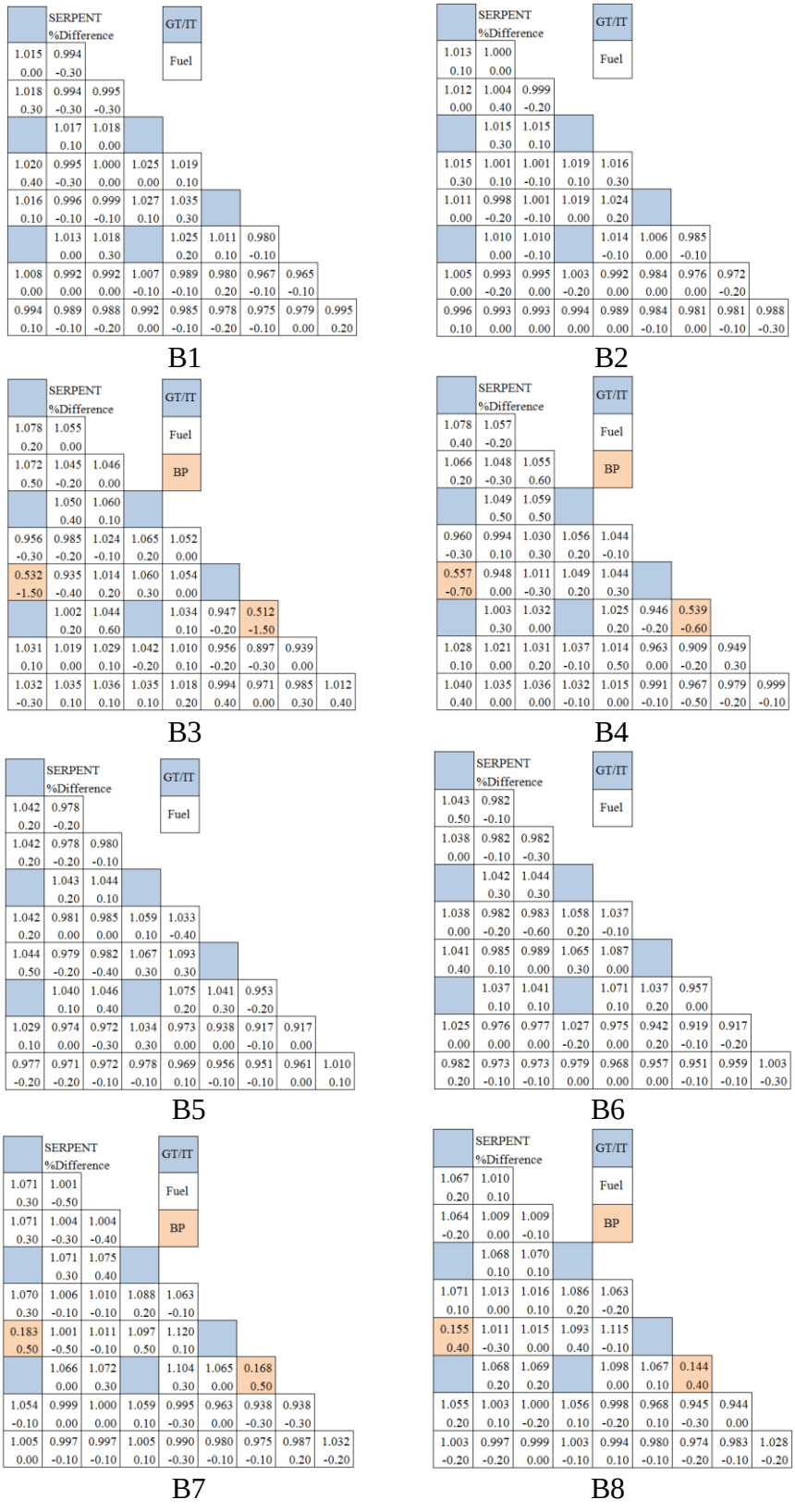

Figure 4. Comparison of pin power distributions.

Table 5. Benchmark results

Case	SERPENT k_{eff}	Reactivity Difference ($\Delta\rho$, *pcm*)				Pin Power Difference (%) (Obtained Using 190-Group Library			
		47-Group		190-Group		Subgroup		ESSM	
		Subgroup	ESSM	Subgroup	ESSM	RMS	Max	RMS	Max
A1	0.22336	-289	-241	-389	-360	-	-	-	-
A2	1.45498	6	124	-9	72	-	-	-	-
A3	1.42268	266	325	340	378	-	-	-	-
A4	1.41442	-32	7	28	52	-	-	-	-
A5	0.20095	-224	-185	-302	-281	-	-	-	-
A6	1.40168	175	221	253	279	-	-	-	-
A7	1.43658	-119	-2	-130	-58	-	-	-	-
A8	1.38204	224	324	319	374	-	-	-	-
B1	1.40457	17	125	-2	73	0.16	0.40	0.17	0.40
B2	1.38919	-111	-5	-125	-59	0.14	0.40	0.14	0.40
B3	1.28614	-77	42	-132	-50	0.35	1.50	0.35	1.50
B4	1.23885	-397	-278	-426	-353	0.28	0.70	0.28	0.70
B5	1.43246	206	258	273	306	0.21	0.50	0.20	0.40
B6	1.41620	173	213	239	263	0.20	0.60	0.20	0.60
B7	1.39653	155	210	221	256	0.25	0.50	0.25	0.50
B8	1.38160	116	160	183	209	0.18	0.40	0.18	0.40

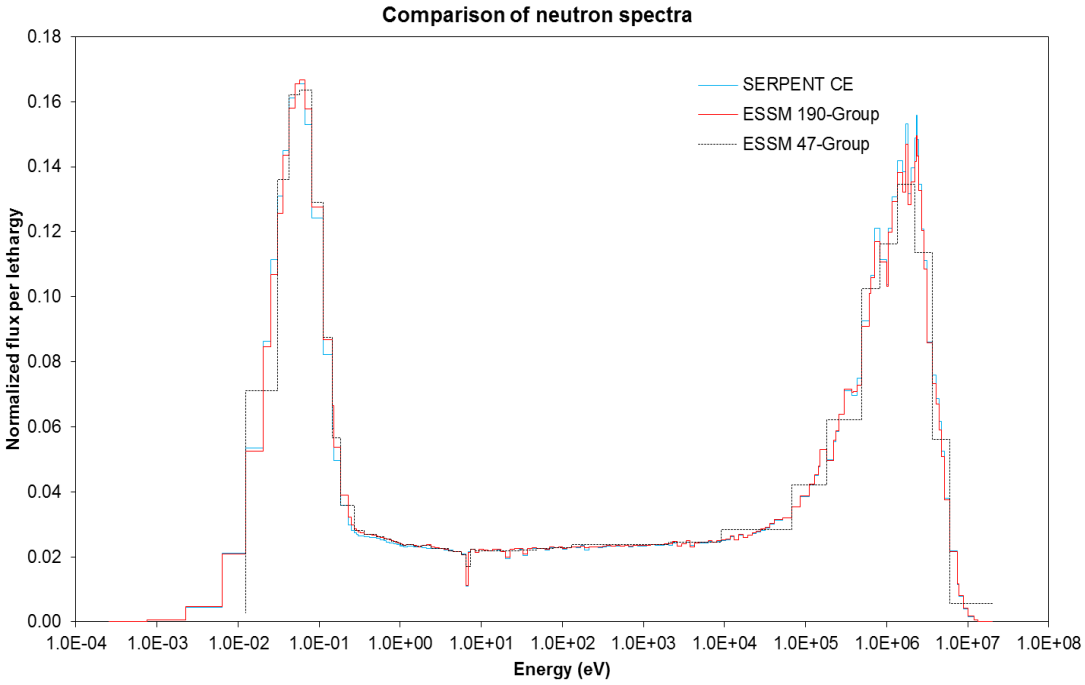

Figure 5. Comparison of neutron spectra for case A2.

4. CONCLUSION

This research focuses on the development of a new fast and robust lattice physics methodology for modeling and simulation of DH nuclear fuels containing TRISO-coated fuel particles and FCM fuel. The Sanchez-Pomraning method for DH calculations could be successfully integrated with the subgroup method and ESSM developed at ORNL for resonance self-shielding calculation and the MOC based eigenvalue calculations. The benchmark results using DH-Subgroup or DH-ESSM and MOC eigenvalue capability based on the Sanchez-Pomraning DH method are very consistent with the reference results obtained using continuous energy Monte Carlo calculations with random distributions of TRISO particles. However, it should be noted that since the cross section libraries including resonance data have been generated only for testing, developing more elaborate cross section libraries for the FCM fuel would enhance the computational accuracy. This will be investigated in the near future.

ACKNOWLEDGMENTS

This research was funded by the ORNL Laboratory Directed Research and Development Programs.

REFERENCES

[1] L. L. Snead et al., *Coated Particle Fuel and Deep Burn Program*, ORNL/TM-2011/125 (2011).

[2] S. G. Hong and K. S. Kim, "Iterative Resonance Treatment Methods Using Resonance Integral Table in Heterogeneous Transport Lattice Calculations," *Ann. Nucl. Energ*. 38, 32–43 (2011).

[3] M. L. Williams and K. S. Kim, "The Embedded Self-Shielding Method," Proc. PHYSOR 2012, Knoxville, Tennessee, USA (2012).

[4] R. Sanchez and G. C. Pomraning, "A Statistical Analysis of the Double Heterogeneity Problem," *Ann. Nucl. Energy* 18, 371 (1991).

[5] R. Sanchez and E. Masiello, "Treatment of the Double Heterogeneity with the Method of Characteristics," Proc. PHYSOR 2002, Seoul, Korea (2002).

[6] R. Sanchez, "Renormalized treatment of the double heterogeneity with the method of characteristics," Proc. PHYSOR 2004, CD-ROM, April 25–29, 2004, Chicago, Illinois, USA (2004).

[7] H. G. Joo et al., "Development of Advanced Suite of Deterministic Codes for VHTR Physics Analysis," KAERI/CM-1021/2006 (2006).

[8] S. G. Hong et al., "Physics study of deep-burning of spent fuel transuranics using commercial LWR cores," *Nucl. Engr. Design* 259, 79–86 (2013).

[9] J. F. Breismeister et al., *MCNP – A General Monte Carlo N-Particle Transport Code Version 4B*, LA-12625-M (1997).

[10] J. Leppänen, R. Mattila, and M. Pusa, "Validation of the SERPENT-ARES Code Sequence Using the MIT BEAVRS Benchmark – Initial Core at HZP Conditions," *Ann. Nucl. Energy* 69, 212–25 (2014).